

## Latent Iron in Silicon

Byoung-Deog CHOI, Dieter K. SCHRODER, Sergei KOVESHNIKOV<sup>1</sup> and Subhash MAHAJAN<sup>2</sup>

Department of Electrical Engineering and Center for Solid State Electronics Research, Arizona State University, Tempe, AZ 85287-5706, U.S.A.

<sup>1</sup>SEH America, Inc., 4111 NE 112th Ave., Vancouver, WA 98682-6776, U.S.A.

<sup>2</sup>Department of Chemical and Materials Engineering and Center for Solid State Electronics Research, Arizona State University, Tempe, AZ 85287-6006, U.S.A.

(Received June 20, 2001; accepted for publication July 23, 2001)

It is usually assumed that the iron in iron-contaminated, boron-doped silicon exists as FeB pairs. The iron can be cycled between its interstitial ( $\text{Fe}_i$ ) and paired ( $\text{FeB}$ ) states with the total density  $\text{Fe}_i + \text{FeB}$  remaining constant. We have discovered that iron can also exist in other paired states, which we believe to be Fe-vacancy or Fe-implant damage pairs. When these pairs are destroyed and subsequently when FeB pairs form, we have observed an increased density. We refer to the excess iron ( $\Delta\text{FeB}$ ) after re-formation as “latent” iron.

KEYWORDS: silicon, iron, impurities, deep-level transient spectroscopy, Fe–B

Iron is one of the most technologically important impurities in silicon. Recent reviews detail many of the effects of Fe in Si and provide numerous references to previous publications.<sup>1,2)</sup> The International Technology Roadmap for Semiconductors requires iron densities below  $10^{10} \text{ cm}^{-3}$  for future Si processing.<sup>3)</sup> Detection of such low iron densities within the Si wafers is possible by several characterization techniques, *e.g.*, surface photovoltage (SPV), photoconductance decay (PCD), and deep-level transient spectroscopy (DLTS).<sup>4)</sup> The former two rely on minority carrier diffusion length and recombination lifetime measurements using the kinetics of Fe–B dissociation in boron-doped silicon as a fingerprint,<sup>5)</sup> while the latter is a direct measurement. Since Fe in boron-doped silicon exists as either Fe–B pairs or as interstitial iron,  $\text{Fe}_i$ , DLTS allows a direct measurement of iron in either one of these states. In this paper we show that these characterization techniques can underestimate the Fe density due to a third iron state—the latent iron. The error can be as high as 100%, which can be critical for today’s silicon, since such device parameters as diode leakage current, gate oxide integrity, and carrier lifetime depend strongly on iron density.

We have discovered a new and previously unreported effect associated with interstitial iron. This is an increase of the iron density in the wafer after annealing, as illustrated in Fig. 1. This figure is a set of DLTS spectra of a Fe-contaminated Si wafer. Trace (a) is the original spectrum after wafer room temperature storage for two years. It clearly shows the well-known FeB peak at  $T = 55.3 \text{ K}$  and essentially no interstitial iron at  $T = 253 \text{ K}$ . After a FeB dissociation anneal at  $180^\circ\text{C}$  for 30 s, the FeB peak disappears and the  $\text{Fe}_i$  peak appears at  $T = 253 \text{ K}$ , as shown by trace (b). The magnitude of the two peaks is approximately the same, as it should be since Fe–B pairs are changed into  $\text{Fe}_i$  and substitutional boron  $\text{B}_s$ . Holding the sample at  $80^\circ\text{C}$  for 15 h followed by room temperature storage for 5 days, causes  $\text{Fe}_i$  and  $\text{B}_s$  to change back into FeB pairs, shown by trace (c). The change from  $\text{Fe}_i$  into FeB pairs is well known. What has not been reported before is the significant increase of the FeB density from the initial  $2 \times 10^{12} \text{ cm}^{-3}$  (trace (a)) to the final  $4.5 \times 10^{12} \text{ cm}^{-3}$  (trace (c)). We call this excess iron “latent iron”, because it was not originally detected as a FeB pair density. What is the source of this excess iron?

We used double side-polished float-zone (FZ), p-type sil-

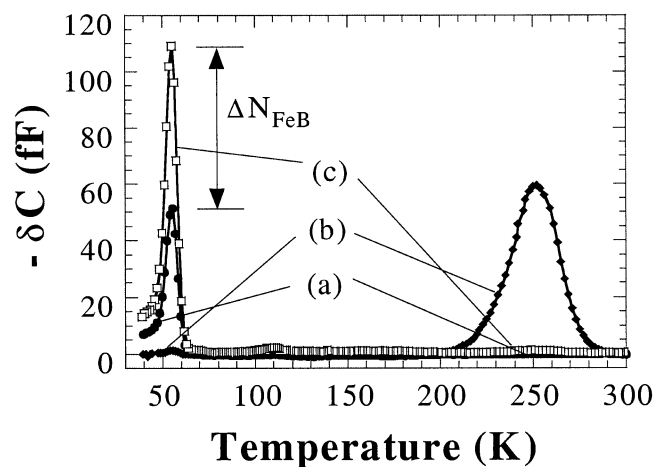
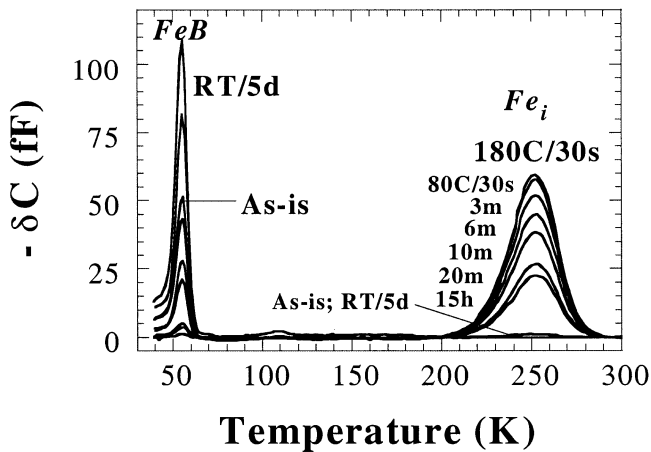


Fig. 1. DLTS spectra of (a) the original sample, (b) after  $180^\circ\text{C}$ , 30 s dissociation anneal, and (c) after  $80^\circ\text{C}/15 \text{ h}$  and room temperature 5 day storage.

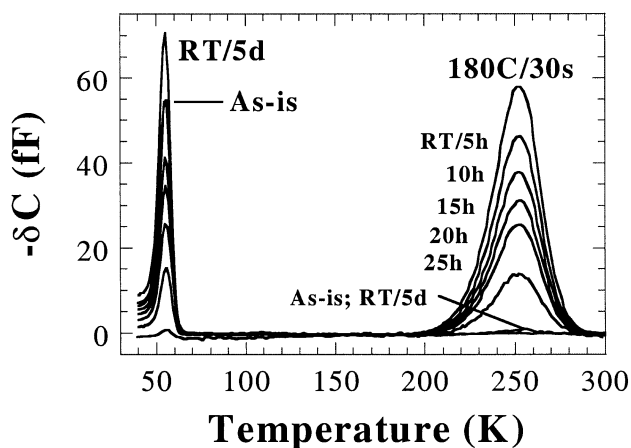
icon wafers doped with boron to  $2.1 \times 10^{14} \text{ cm}^{-3}$ . Iron was introduced by thermal annealing at  $900^\circ\text{C}$  for 2 hours following iron implantation into the back surface with a dose of  $10^{11} \text{ cm}^{-2}$  and energy of 100 keV. DLTS measurements on the front wafer surface yielded an iron density of  $2 \times 10^{12} \text{ cm}^{-3}$ . Schottky diodes were fabricated by aluminum-evaporated contacts on the front surface and a large-area silver paste contact on the back surface. The samples were characterized with current–voltage, capacitance–voltage, and DLTS measurements.

Capacitance–voltage data showed little change before and after dissociation anneal. This is expected since the effective doping density change, due to boron becoming inactive in the FeB state and active in the unpaired FeB state, is very small because the iron density ( $\sim 10^{12} \text{ cm}^{-3}$ ) is much lower than the boron density ( $\sim 10^{14} \text{ cm}^{-3}$ ). Schottky diode current–voltage measurements showed a substantial current and diode ideality factor change upon dissociation anneal, possibly associated with changes at the metal/Si interface.

The key DLTS results are shown in Figs. 2(a) and 2(b). The samples were initially measured after storage at room temperature for 2 years. This is the “As-is” curve in both figures. Then they were annealed at  $180^\circ\text{C}/30 \text{ s}$  to dissociate the Fe–B pairs. The FeB peak vanished and the  $\text{Fe}_i$  peak



(a)

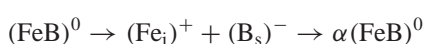


(b)

Fig. 2. DLTS spectra for "As-is", after 180°C/30 s dissociation anneal and (a) 80°C storage for various times followed by room temperature/5 days, (b) room temperature storage for various times.

appeared. The wafer in Fig. 2(a) was then annealed at 80°C for various times up to 15 h and DLTS spectra were recorded. Then the sample was held at room temperature for five days and a last DLTS spectrum was taken. The  $Fe_i$  peak has essentially disappeared and the  $Fe_B$  peak has reappeared, but it is significantly higher than the original. The sample in Fig. 2(b) underwent a dissociation anneal as that in 2(a), but was held at room temperature thereafter, instead of at 80°C, and DLTS spectra were recorded. The results are qualitatively similar to those in Fig. 2(a). Note that the magnitude of the "As-is" Fe-B peak and the  $Fe_i$  peak immediately after the dissociation anneal are about the same. It is only after an extended time at room temperature or 80°C that the latent iron appears in the new Fe-B peak. The initial 180°C/30 s dissociation anneal is insufficient to generate the latent iron.

In both cases we note the  $Fe_B$  density to be higher after this anneal sequence than at the start. This "latent" iron, denoted as  $\Delta N_{FeB}$  in Fig. 1, is higher for the 80°C anneal than for the room temperature anneal case. We express this sequence as



with  $\alpha$  between 1 and 3. For the  $T = 80^\circ\text{C}$  anneal,  $\alpha \approx 2$ . The temporal behavior is shown in Fig. 3 for the 80°C anneal case. The  $Fe_B$  density starts out at  $2 \times 10^{12} \text{ cm}^{-3}$ , drops to approximately zero after the 180°C/30 s anneal, then gradually increases and begins to saturate at  $5.4 \times 10^4 \text{ s}$  (15 h), the limit of our measurement. After storing the sample at room temperature for 5 days,  $N_{FeB}$  increases further.  $\Delta N_{FeB}$ , defined as the final density minus the initial density, is plotted versus anneal temperature in Fig. 4. It remains reasonably constant, then increases rapidly at around 70°C and appears to saturate around 80–90°C. For each datum point in Fig. 4,  $\Delta N_{FeB}$  is defined as in Fig. 3. At this point we do not understand the rapid  $\Delta N_{FeB}$  increase from 70°C to 80°C. From Fig. 3 it appears the additional 5 day room temperature anneal contributes significantly to this increase.

It is generally assumed that all of the iron in boron-doped Si is complexed with boron after storage at room temperature for a few days or longer.<sup>6–8)</sup> However, in addition to boron, there may be other possible sinks for iron. Two of these are growth-induced thermal vacancies, and ion implantation-induced damage. Since vacancies can be negatively charged in silicon, they may have Coulombic interaction with positively charged  $Fe_i$ . Furthermore,  $Fe_i^+ - V$  pairing may be facilitated by the difference in covalent tetrahedral radii of Fe and Si atoms. A simple calculation shows that the density of thermal vacancies after a 900°C anneal is sufficiently high to

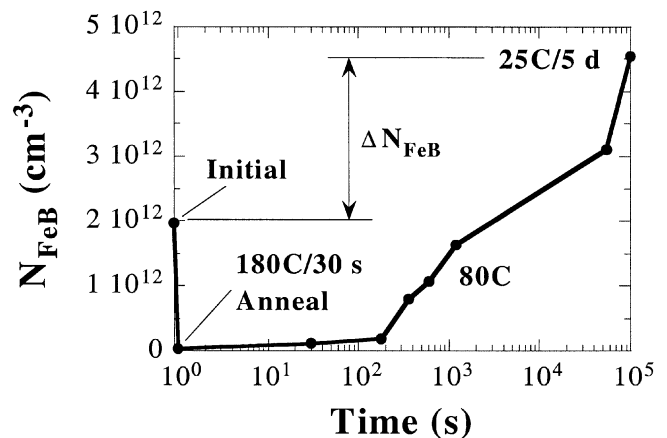


Fig. 3.  $N_{FeB}$  as a function of time following various anneals.

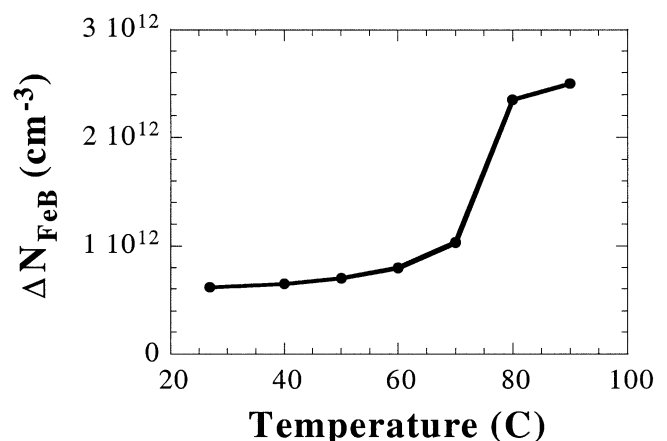


Fig. 4.  $\Delta N_{FeB}$  as a function of anneal temperature. The time for each temperature was 15 h at each temperature + 5 days at room temperature.

bond with  $2 \times 10^{12} \text{ cm}^{-3}$  iron atoms.

Since Fe was introduced in our samples by ion implantation at 100 keV, it is possible that implantation-induced damage occurred in the wafers. This damage could consist of silicon vacancies and interstitials. The majority of these point defects may be annihilated during the 900°C anneal, but some of them may cluster in the form of microdefects or dislocation loops to serve as sinks for iron. The implant created vacancies are generated at the side opposite to the DLTS measurements. The vacancy diffusion coefficient is difficult to determine, but has been given as  $10^{-5} \text{ cm}^2/\text{s}$  at 1100°C with an activation energy of 0.35 to 0.45 eV.<sup>9,10)</sup> These values lead to a diffusion coefficient of about  $5 \times 10^{-6} \text{ cm}^2/\text{s}$  at 900°C, giving a  $(2Dt)^{1/2}$  diffusion length of 2700  $\mu\text{m}$ , more than sufficient to diffuse through our 700  $\mu\text{m}$  thick wafers. The iron was introduced by thermal annealing at 900°C for 2 hours following iron implantation.

We envisage that during the 180°C anneal, some of the iron atoms may be released from the two types of sinks and become available to form FeB pairs. Even though we are not able to distinguish between the two possible sinks, we feel that ion implantation-induced damage may dominate as a trap for iron atoms because it is more extensive. Interestingly, these pairs do not appear on the DLTS plots over the temperature range of 40–300 K, because they cannot be detected by DLTS or their energy level is such that it is not accessible in the temperature range scanned in the DLTS measurements.

To summarize, we have observed iron in boron-doped Si that we believe to be paired with defects rather than with boron. First, we determine the density of FeB pairs, then dissociate these pairs by a 180°C/30 s anneal and store the samples sufficiently long to reform FeB pairs. The reformed FeB pair density is higher by a factor of two or more than the initial density. We believe the Fe-defect pairs to be either Fe-vacancy or Fe-implant damage pairs.

The research leading to this paper was partially funded by the Silicon Wafer Engineering and Defect Science Consortium (SiWEDS) (Intel, Komatsu Electronic Metals, LG Siltron, MEMC Electronic Materials, Mitsubishi Silicon, Okmetic, Sumitomo Sitix Silicon, Texas Instruments, and Wacker Siltronic Corp.).

- 1) A. Istratov, H. Hieslmair and E. Weber: *Appl. Phys. A* **69** (1999) 13.
- 2) A. Istratov, H. Hieslmair and E. Weber: *Appl. Phys. A* **70** (2000) 489.
- 3) Semiconductor Industry Association (SIA), *The International Technology Roadmap for Semiconductors*, Semiconductor Industry Association, 1999.
- 4) D. K. Schroder: *Semiconductor Material & Device Characterization* (Wiley-Interscience, New York, 1998) 2nd ed.
- 5) G. Zoth and W. Bergholz: *J. Appl. Phys.* **67** (1990) 6764.
- 6) K. Graff and H. Pieper: *J. Electrochem. Soc.* **128** (1981) 669.
- 7) L. C. Kimerling and J. L. Benton: *Physica* **B116** (1983) 297.
- 8) W. Wijaranakula: *J. Electrochem. Soc.* **140** (1993) 275.
- 9) R. Falster and V. V. Voronkov: *Mater. Sci. Eng.* **B73** (2000) 87.
- 10) G. Watkins: *Mater. Sci. Semicond. Proc.* **3** (2000) 227.